

# Deuteron Electro-Disintegration at Very High Missing Momenta

K. Aniol

*California State University L.A.*

F. Benmokhtar

*Carnegie Mellon University*

W.U. Boeglin (spokesperson), P.E. Markowitz, B.A. Raue,  
J. Reinhold and M. Sargsian

*Florida International University*

C. Keppel, M. Kohl

*Hampton University*

D. Gaskell, D. Higinbotham, M. K. Jones (co-spokesperson), G. Smith and  
S. Wood

*Jefferson Lab*

S. Jeschonnek

*Ohio State University*

J. W. Van Orden

*Old Dominion University*

G. Huber

*University of Regina*

E. Piasetzky, G. Ron, R. Shneor

*Tel-Aviv University*

H. Bitao

*Lanzhou University*

X. Jiang, A. Puckett

*Los Alamos National Laboratory*

S. Danagoulian

*North Carolina A&T State University*

H. Baghdasaryan, D. Day, N. Kalantarians, R. Subedi

*University of Virginia*

F. R. Wesselmann

*Xavier University of Louisiana*

A. Asaturyan, A. Mkrtchyan, H. Mkrtchyan, V. Tadevosyan and

S. Zhamkochyan

*Yerevan Physics Institute*

### Abstract

We propose to measure the  $D(e,e'p)n$  cross section at  $Q^2 = 4.25$   $(\text{GeV}/c)^2$  and  $x_{bj} = 1.35$  for missing momenta ranging from  $p_m = 0.5$   $\text{GeV}/c$  to  $p_m = 1.0$   $\text{GeV}/c$  expanding the range of missing momenta explored in the Hall A experiment (E01-020). At these energy and momentum transfers, calculations based on the eikonal approximation have been shown to be valid and recent experiments indicated that final state interactions are relatively small and possibly independent of missing momenta. This experiment will provide for the first time data in this kinematic regime which are of fundamental importance to the study of short range correlations and high density fluctuations in nuclei. The proposed experiment could serve as a commissioning experiment of the new SHMS together with the HMS in Hall C. A total beam time of 21 days is requested.

# 1 Contribution to the Hall C Upgrade

Werner Boeglin and Joerg Reinhold plan to contribute to the Hall C Analysis Software development. Werner Boeglin has previously contributed to the old Hall A analyzer ESPACE and participated in numerous Hall C experiment as run coordinator. Starting with the first Hall C experiments in 1995/96 Joerg Reinhold has not only managed numerous experiments as run coordinator and spokesperson, but also coordinated the corresponding analysis efforts. Thus, he has extensive knowledge of the existing Hall C software down to the source code level. He already started discussions with the SHMS-HMS User Board on how he could contribute. More firm tasks will be assigned during the next Hall C meeting in January 2010.

Pete Markowitz reaffirms his previously made commitment to work on the SHMS commissioning, as well as the software and data acquisition upgrades. The SHMS will require verification of the optics and measurements of acceptance and detector efficiencies. He has previously worked on the Halls A and C spectrometer commissioning and software for Hall A analysis.

## 2 Physics Motivation

High-energy, exclusive electro-disintegration of the deuteron is considered as the most effective process in probing two nucleon dynamics at short space time distances. The latter condition is essential for probing the limits of nucleonic degrees of freedom in strong interaction dynamics.

Recently, several electro-production experiments involving  $A > 2$  nuclei[1, 2, 3, 4] clearly demonstrated the possibility of probing high momentum components at high  $Q^2$  and  $x_{bj} > 1$  kinematics. These experiments prepare the stage for the exploration of nuclear structure at short distances which is of fundamental importance in understanding the limits of the nucleonic picture of nuclei and the dynamics of the nuclear force at short distances. However, the most basic system to study in this respect is the deuteron as many questions related to two-nucleon short range correlations are directly related to high values of relative momenta in the  $NN$  system. The best way to probe large relative momenta in the  $NN$  system is to study deuteron electro-disintegration at the same kinematics in which the above mentioned  $eA$  reactions are studied.

After an initial deuteron break-up experiment[11] was carried out at a moderate value of  $Q^2 = 0.66$  (GeV/c)<sup>2</sup>, two new experiments at Jefferson Lab[12, 13, 14] for the first time probed deuteron break-up at large  $Q^2$  kinematics. They supported the claim that high  $Q^2$  and  $x_{bj} > 1$  are necessary conditions for using the deuteron break-up reaction as an effective tool for the investigation of large relative momenta in the  $pn$  system. This claim was based on the theoretical expectation that at these kinematics soft, two-body processes are either suppressed (such as meson exchange currents and isobar contributions) or under the control (final state interactions).

Currently no data exist that satisfy this condition for missing momenta above  $p_m = 0.5$  GeV/c. Data in this kinematic range are of fundamental interest not only for the short range structure of the deuteron itself, but also for the interpretation of future experiments that probe the structure of short range correlations in heavier nuclei. In recent years considerable progress has been made in the development of theoretical methods for the calculation of high  $Q^2$  electro-disintegration of two and three nucleon systems [5, 6, 7, 8, 9, 10] extending the possibility of investigating the bound nucleon's momentum range beyond  $p_m = 0.5$  GeV/c.

### 2.1 Research Subjects in Deuteron Electro-Disintegration

Probing the deuteron at large relative momenta via electro-disintegration will make contributions to addressing several issues, each of them having a funda-

mental importance in nuclear physics.

- **Reaction Dynamics:** At large internal momenta, the virtual photon interacts with a deeply bound nucleon whose interaction dynamics is largely unknown. The research subjects include the structure of the electromagnetic current as well as modifications of nucleon form factors due to large off-shell effects. The latter is part of the wider program of studies of modification of hadrons in the nuclear medium.
- **Final State Interaction:** In the break-up reaction, the proton and neutron undergo strong final state interactions (FSI). The contribution of FSI can not be neglected and its understanding is an important condition for the success in probing the deuteron at small  $pn$  separations. The advantage of high  $Q^2$  is that one can satisfy the condition of eikonicity of the final state interaction which allows one to sum the large number of partial waves in the  $pn$  continuum into the elastic  $pn$  scattering amplitude. The eikonal nature of FSI is characterized by a very specific angular dependence of the deuteron break-up reaction as a function of the neutron recoil angle which can be studied experimentally.
- **Deuteron Wave Function:** Finally one of the most fundamental aspects of studies of the deuteron break-up reaction is to probe the deuteron wave function at small inter-nucleon distances. This is related to the understanding of several issues such as the  $NN$  potential at short distances, relativistic effects and non-nucleonic components as well as the transition from hadronic to quark-gluon degrees of freedom in the strongly bound  $pn$  system.

The above discussed research subjects are intertwined. The advantage of the exclusive break-up reaction is that it provides a multitude of observables and kinematic settings that can be used to ultimately separate the various processes considered. These observables include  $Q^2$ ,  $x$ , recoil momentum and angular dependence of the break-up cross section as well as the measurement of asymmetries when polarization degrees of freedom are included.

## 2.2 Experimental Status

A previous Hall A experiment determined the  $D(e,e'p)n$  cross section at a relatively low momentum transfer of  $Q^2 = 0.67$  (GeV/c)<sup>2</sup> for missing momenta up to  $p_m = 0.55$  GeV/c at  $x_{bj} \approx 1$  [11]. Even though the measured  $Q^2$  was relatively small, the momentum of the final proton was 1 GeV/c which

was large enough for the eikonal approximation to be valid. Figs. 1 and 2 show the comparisons of two different models[5, 10] with the data and both indicate that at this kinematic setting ( $x \approx 1$ ) final state interactions strongly dominate the cross section especially for missing momenta above 0.4 GeV/c. Both calculations also show that FSI are reasonably under the control.

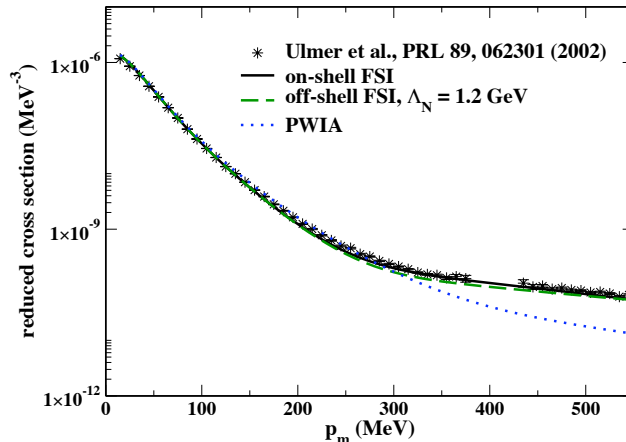


Figure 1: The reduced cross section for a beam energy of 3.1095 GeV,  $Q^2 = 0.665$  (GeV/c) $^2$ ,  $x_{Bj} = 0.964$ , and  $\phi_p = 180^\circ$ . The data are from [11].

This has been confirmed by two recently completed experiments[12, 13, 14] at Jefferson Lab representing the first attempts to systematically study the exclusive deuteron break-up reactions in the  $Q^2 \geq 1$  (GeV/c) $^2$  region. They also confirmed that meson-exchange currents are a small correction to the overall cross section and that isobar currents can be kept under control by choosing  $x_{bj} > 1$ [14].

An important result of these experiments was that even though the final state interaction in many cases is not small it can be understood quantitatively (Figs. 3,4,5). Already at  $Q^2 \geq 2$  (GeV/c) $^2$  the eikonal regime is established which allows one to perform increasingly reliable estimates of these effects. Also these experiments for the first time confirmed the prediction of the eikonal approximation[15, 16] that the maximum of FSI corresponds to the recoil angle of around  $70^\circ$ . This situation gives us some confidence that we can move beyond FSI to investigate the other characteristics of the deuteron-break up reaction. Note, a one-to-one relation exists between the angle of the recoiling neutron ( $\vartheta_{nq}$ ) relative to the momentum transfer and  $x_{bj}$  where an increasing  $x_{bj}$  corresponds to a decreasing  $\vartheta_{nq}$ .

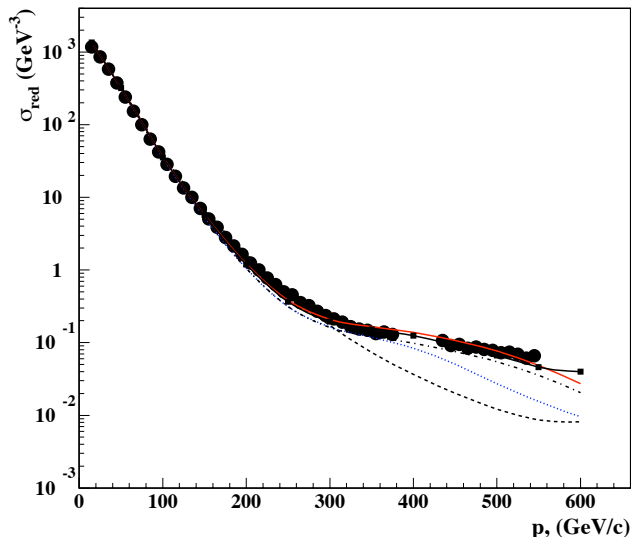


Figure 2: Missing momentum dependence of the reduced cross section. The data are from Ref.[11]. Dashed line - PWIA calculation, dotted line - PWIA+ only pole term of forward FSI, dash-dotted line - PWIA+ forward FSI, solid line - PWIA + forward and charge exchange FSI, and solid line with squares - same as the previous solid line, added the contribution from the mechanism in which the proton is a spectator and the neutron was struck by the virtual photon

### 2.3 Goal of the Proposal

From the theoretical point of the view, the most intriguing question is how far one can extend the boundaries of the theoretical framework based on the description of the deuteron as a two-nucleon system? This question can be answered only if one starts to probe the deuteron at extreme kinematics corresponding to very large initial momenta of nucleons in the deuteron.

In the CLAS experiment, cross sections for large recoil momenta have been determined, however it was necessary to integrate over a wide range of momentum transfers ( $1 (\text{GeV}/c)^2$ ) and neutron recoil angle ( $0^\circ - 180^\circ$ ). As a consequence the reaction dynamics is not well defined for these experimental cross sections and at recoil momenta above  $0.5 \text{ GeV}/c$  the cross sections are completely dominated by final state interactions.

As we will argue in this proposal, the experience we gained from the two recent JLab experiments allows us for the first time to push our studies to the significantly unexplored kinematic domain of probing missing momenta up to



1 GeV/c at  $Q^2 = 4.25$  (GeV/c)<sup>2</sup> with a kinematic setting that is well defined, minimizes final state interactions, MEC and IC, and suppresses the indirect reaction where the neutron is hit and one observes the recoiling proton.

## 2.4 Proposed Measurement

In this proposal we plan to perform an exploratory measurement of the:

$$e + d \rightarrow e' + p + n \quad (1)$$

reaction probing missing momenta up to 1 GeV/c for one setting of  $Q^2$  and  $x_{bj}$ . It will be for the first time that high  $Q^2$  deuteron break up is probed in electro-production at such large missing momenta and momentum transfer, at a well defined kinematic setting. To interpret this experiment we will use three important theoretical observations [15, 16, 17, 18, 19] which the previous two experiments[12, 13] confirmed:

- Generalized eikonal approximation (GEA) is an appropriate theoretical framework for the description of the reaction [1] at  $Q^2 > 1$  (GeV/c)<sup>2</sup>. These experiments confirmed that the FSI is uniquely defined by the missing momenta of the reaction: being dominated by screening effects at  $p_m \leq 200$  MeV/c and dominated by pure re-scattering effects at  $p_m > 300$  MeV/c. (See Fig. 6.)
- At  $p_m \geq 400$  MeV/c, the peak of re-scattering is at  $\theta_{recoil} = 70^\circ$  as predicted within GEA[15] and not at  $90^\circ$  was expected within conventional Glauber approximation. (See Fig 6.)
- The eikonal nature of FSI creates a unique angular dependence of the FSI effects. It is an interplay of screening (interference of PWIA and FSI amplitudes) and re-scattering (square of FSI amplitude) effects which enter with an opposite sign in the cross section of the reaction. The decrease of re-scattering effects at forward and backward recoil angles is associated with the increase of the interference effects. Since both effects are defined by the same re-scattering NN amplitude one arrives at approximate recoil momentum independence of the recoil angles at which these two effects significantly cancel each other. (See Fig. 7.)

The last point of the above observation opens a rather unexpected window to probe the deuteron at very high missing momenta. As it follows from Fig. 7, this corresponds to the recoil angles  $\vartheta_{nq} = \theta_r \approx 40 \pm 5^\circ$  for which FSI effects are confined within  $\approx 30\%$  for missing momenta up to 0.95 GeV/c. This value of  $\vartheta_{nq}$  corresponds to a value of  $x_{bj} \approx 1.35$ .

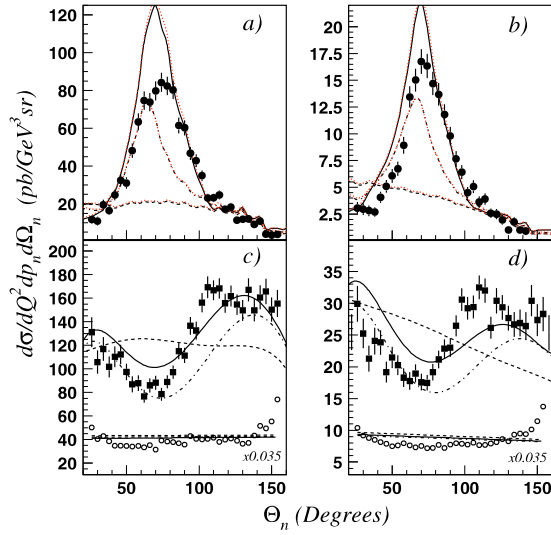


Figure 3: Angular distribution of recoiling neutrons measured in CLAS for (a)  $Q^2 = 2 \pm 0.25$  (GeV/c) $^2$ ,  $400 < p_n < 600$  MeV/c, (b)  $Q^2 = 3 \pm 0.5$  (GeV/c) $^2$ ,  $400 < p_n < 600$  MeV/c, (c)  $Q^2 = 2 \pm 0.25$  (GeV/c) $^2$ ,  $200 < p_n < 300$  MeV/c, (d)  $Q^2 = 3 \pm 0.5$  (GeV/c) $^2$ ,  $200 < p_n < 300$  MeV/c. The data for  $p_n < 100$  MeV/c are plotted in the bottom part of (c) and (d), scaled by 0.035. The dashed, dashed-dotted and solid curves are calculations with the Paris potential using PWIA, PWIA+FSI and PWIA+FSI+MEC+IC respectively [14].

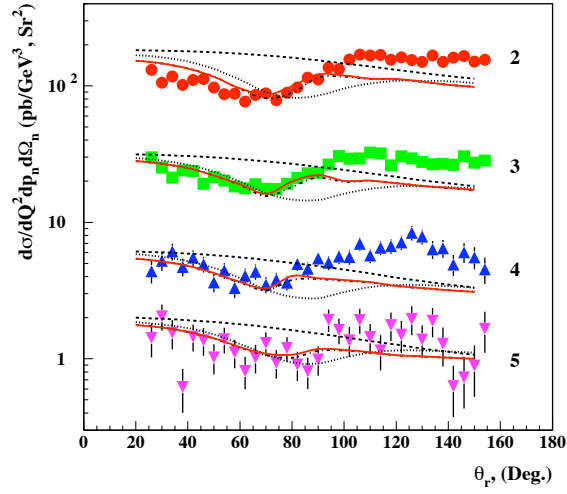


Figure 4: Dependence of the differential cross section on the direction of the recoil neutron momentum. The data are from Ref.[14]. Dashed line - PWIA calculation, dotted line - PWIA+ pole term of forward FSI, dash-dotted line - PWIA+forward FSI, solid line - PWIA + forward and charge exchange FSI. The momentum of the recoil neutron ( $p_m$ ) is restricted to  $200 \ll 300$  MeV/c. The labels 2, 3, 4 and 5 correspond to the following values of  $Q^2 = 2 \pm 0.25; 3 \pm 0.5; 4 \pm 0.5; 5 \pm 0.5$  (GeV/c) $^2$ . No IC is included in the calculations.

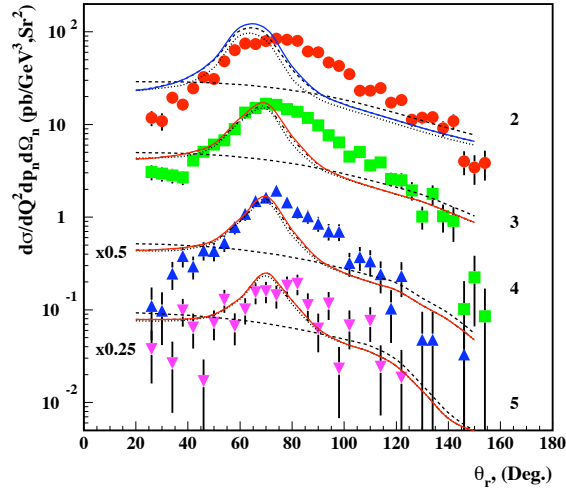


Figure 5: Dependence of the differential cross section on the direction of the recoil neutron momentum. The data are from Ref.[14]. Dashed line - PWIA calculation, dotted line - PWIA+ pole term of forward FSI, dash-dotted line - PWIA+forward FSI, solid line - PWIA + forward and charge exchange FSI. The momentum of the recoil neutron is restricted to  $400 < p_m < 600$  MeV/c. The labels 2, 3, 4 and 5 correspond to the following values of  $Q^2 = 2 \pm 0.25; 3 \pm 0.5; 4 \pm 0.5; 5 \pm 0.5$  (GeV/c)<sup>2</sup>. The data sets and calculations for “4” and “5” are multiplied by 0.5 and 0.25 respectively. No IC is included in the calculations.

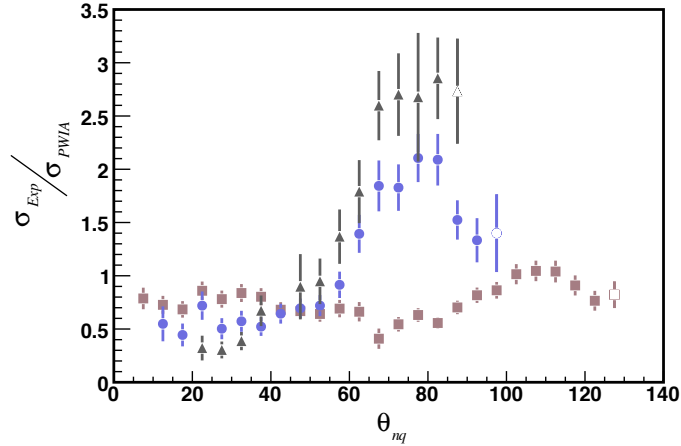


Figure 6: The ratio  $R = \sigma_{Exp}/\sigma_{PWIA}$  from the Hall A experiment E01-020 as a function of the recoil neutron angle  $\vartheta_{nq}$  [42] for  $p_m = 200$  MeV/c ( filled brown squares),  $p_m = 400$  MeV/c ( filled purple circles),  $p_m = 500$  MeV/c ( filled black triangles). One can see that around  $\vartheta_{nq} = 40^\circ$  the effect of FSI does not depend strongly on  $p_m$ .

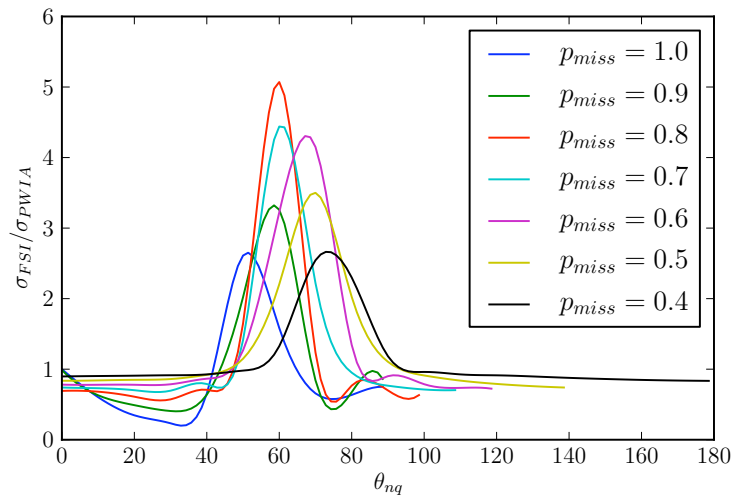


Figure 7: The ratio  $R = \sigma_{FSI}/\sigma_{PWIA}$  calculated for missing momenta ranging from 0.4 GeV/c up to 1.0 GeV/c and using the Paris potential. The black curve corresponds to  $p_m = 0.4$  GeV/c and the ratio R is maximal close to  $80^\circ$  while the blue curve corresponds to 1 GeV/c and R for this value is maximal at about  $50^\circ$ . One can therefore see that in a region around  $\vartheta_{nq} = 40^\circ$  the effect of FSI is only slightly dependent on  $p_m$  and within  $\approx \pm 30\%$ .

## 2.5 What can be learned from these measurements?

Being able to confine FSI effects within 30% and pushing the measurements up to  $p_m = 1$  GeV/c will allow us for the first time to probe the sensitivity of the scattering process to the (i) Reaction dynamics (ii) Deuteron wave function and (iii) Non-nucleonic degrees of freedom.

### 2.5.1 Reaction Dynamics

The description of the electromagnetic interaction with bound (off-shell) nucleons possesses many theoretical uncertainties. The origin of the off-shell effects in the  $\gamma^* N_{bound}$  scattering amplitude is somewhat different for low and high energy domains. In the case of low energy transfer, the nucleons represent the quasi-particles whose properties are modified due to the in-medium nuclear potential (see e.g. [27]). At high  $Q^2$ , the virtual photon interacts with nucleons and the phase space volume of the process is sufficiently large. As a result, the off-shell effects in the high energy limit are mostly related to the non-nucleonic degrees of freedom. Several approaches exist to treat the off-shell effects in the high energy limit. One of the frequently used models is the virtual nucleon approximation (see e.g. [28, 29, 16], in which the scattering is described in the LAB frame of the nucleus and electrons scatter off the virtual nucleon whose virtuality is defined by the kinematic parameters of the spectator nucleon. In this case the form of the wave function is defined through the evaluation of the amplitude at the one-mass shell pole of the spectator nucleon propagator in the Lab frame. This yields an off-energy-shell state of the bound nucleon.

### 2.5.2 Deuteron Wave Function

Our knowledge of the deuteron wave function is restricted up to 400 MeV/c relative momentum. Wave functions based on different NN potentials start to diverge beyond this momentum range. The uncertainty of the deuteron wave function is not only related to the uncertainties of the NN potential. The problem is more conceptual in a sense that the many potentials constructed in configuration space are based on the local (static) approximation and become less and less relevant with the increase of the relative momenta of the interacting nucleon. Staying within the framework of nucleonic degrees of freedom this issue is related to the accounting for the relativistic effects in two-nucleon systems. These effects are significant in the region influenced by the core of the NN interaction.

The two points discussed above are based on the nucleonic picture of both interaction dynamics and nuclear wave function. These approximations have

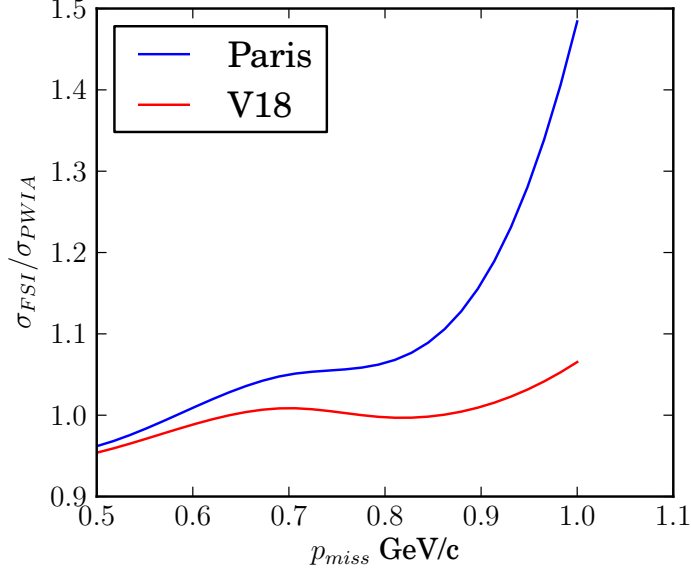


Figure 8: The cross section ratio  $\sigma_{FSI}/\sigma_{PWIA}$  for  $x_{bj} \approx 1.35$  using the Paris potential (blue line) and the V18 (red line), illustrating the contributions of FSI. For  $p_m \leq 0.95$  GeV/c for both models these contributions are below 30%

never before been applied to the large  $Q^2$  kinematics when very large missing momenta are probed. One expects that at some point these approximations should fail qualitatively similar to what happened in high energy large angle photo-disintegration reactions of the deuteron[30, 31, 32, 33, 34]. The proposed experiment may answer at which kinematics such a breakdown occurs.

### 2.5.3 Non-nucleonic degrees of freedom

Theoretically one expects that with a recoil energy exceeding the pion-threshold, the contributions due to non-nucleonic degrees of freedom should become increasingly important. To date there are only very few nuclear experiments[30, 31, 32, 33, 34] for which such a transition is clearly observed. These experiments played a very significant role in the advancement of different theoretical approaches that explicitly take into account quark-degrees of freedom in the nuclear interaction[35, 36, 37]. Deuteron electro-disintegration with 1 GeV/c recoil momentum will be one of such experiments.

We don't expect to resolve all the above issues with one such measurement. However, this measurement will be the first in which the kinematics are taken

to the limit where a transition to non-nucleonic degrees of freedom is expected.

## **2.6 Theoretical support of these studies**

The above mentioned experiments[12, 13] generated significant interest in new theoretical studies of high energy electro-disintegration processes. Several theoretical groups now are working on the theory of high energy deuteron electro-disintegration (e.g. [20, 21, 22, 23, 24, 25]). These groups established the benchmarking collaboration to verify the agreement of their calculations at more conventional kinematic situations[26]. Assuming that these groups agree at low missing momentum kinematics, their comparisons with the data at very large missing momenta will allow one to set the limits on how much the approximations based on nucleonic degrees of freedom can account for the cross section of the reaction.



### 3 Experimental Program

We plan to measure the  $D(e,e'p)n$  cross section at kinematic settings centered on the following missing momenta:  $p_m = 0.5, 0.6, 0.7, 0.8, 0.9$  and  $1.0$  GeV/c. Electrons will be detected in SHMS and the ejected protons in HMS. For each setting the electron arm will remain unchanged and the electron kinematics will be fixed at  $Q^2 = 4.25$  (GeV/c)<sup>2</sup> and  $x_{bj} = 1.35$ .

Measurements will be done at  $p_m = 0.1$  GeV/c for  $Q^2 = 3.5$  (GeV/c)<sup>2</sup> and  $Q^2 = 4.25$  (GeV/c)<sup>2</sup>. These data will be used for normalization measurements since at this value of  $p_m$  contributions of FSI, MEC and IC are small and the cross sections are large. This has been confirmed by measurements at much lower  $Q^2$  values [39, 40, 41]. In addition, we will also measure the  $^1\text{H}(e,e'p)$  hydrogen elastic reaction as a cross check of spectrometer acceptance models, an additional study of target boiling effects and a systematic check of error in beam energy, spectrometer's central momentum and angle setting using the kinematics of the elastic reactions.

Fig. 6 shows the ratio between the experimental  $D(e,e'p)n$  cross section determined in the E01-020 experiment [42] and the calculated one using PWIA (using MCEEP and the PWIA model of S. Jeschonnek). For  $p_m = 0.5$  GeV/c large FSI effects exist at  $\vartheta_{nq} \approx 70^\circ$  ( $x_{bj} \approx 1$ ) as well as for  $\vartheta_{nq} \leq 35^\circ$  ( $x_{bj} \geq 1.5$ ). For angles larger than  $100^\circ$  the energy transfer is increasing ( $x_{bj}$  is decreasing) and one expects increasing contributions of isobar currents.

In Fig. 6, one can see that at a neutron recoil angle of about  $40 - 45^\circ$ , corresponding to a value of x-Bjorken of  $x_{bj} \approx 1.3$ , the effects of FSI are reduced to 20 - 30% and seem to depend only weakly on the recoil momentum. This phenomenon is reproduced by the calculation of M. Sargsian (Fig. 7). The estimated FSI effect as a function of missing momentum for a fixed value of  $x_{bj} \approx 1.35$  is illustrated in Fig. 8 by the ratio  $R = \sigma_{FSI}/\sigma_{PWIA}$ . It is due to this observation that we selected the electron kinematics. The following criteria determined the selection of the momentum transfer:

- The momentum transfer has to be large enough for GEA to be applicable
- The final proton momentum has to be significantly larger than the neutron recoil momentum in order to suppress the indirect reaction where the struck particle is the neutron and the observed proton is the recoiling spectator. As shown previously the interference of these two processes leads to a reduction of the cross section.

The relation between the momentum vectors for the direct and the indirect reaction are illustrated in Fig. 9 for  $p_m = 0.5, 0.7$  and  $1.0$  GeV/c. Fig. 9a shows

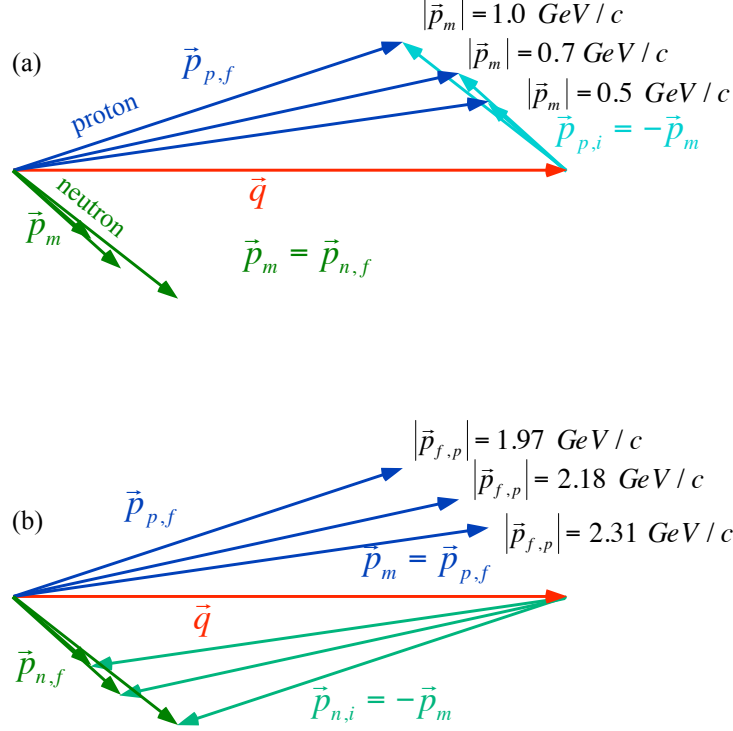


Figure 9: The momentum vectors for the direct proton knockout (a) and for the indirect reaction (b) where the proton is the spectator and the neutron absorbs the virtual photon.

the direct reaction where the proton with an initial momentum of  $p_m = 0.7$  GeV/c absorbs the virtual photon and is ejected with a final momentum of  $p_f = 2.18$  GeV/c. For the indirect reaction (shown in Fig. 9b), a neutron with in initial momentum of 2.18 GeV/c absorbs the photon and the recoiling proton is observed. We expect that the probability to find a nucleon with an initial momentum of 2.18 GeV/c is considerably smaller compared to the one of finding a nucleon with an initial momentum of 0.7 GeV/c. Overall the ratio between the final nucleon momentum and the recoil momentum is always larger than 1.9 in all kinematic settings and consequently we do not expect an effect of the indirect reaction of more than about 10%. The detailed kinematics can be found in Tab. 1. The acceptance in missing momentum for each kinematic setting is shown in Fig. 10.

$p_m$	$E_f$	$\vartheta_e$	$ \vec{q} $	$p_f$	$\vartheta_p$	$\vartheta_{pq}$	$\vartheta_{nq}$
0.5	9.322	11.68	2.658	2.305	53.47	8.21	41.19
0.6	9.322	11.68	2.658	2.251	55.60	10.34	42.31
0.7	9.322	11.68	2.658	2.189	57.63	12.37	42.06
0.8	9.322	11.68	2.658	2.121	59.61	14.35	41.07
0.9	9.322	11.68	2.658	2.047	61.56	16.30	39.67
1.0	9.322	11.68	2.658	1.969	63.49	18.23	38.02

Table 1: Central kinematic settings for the proposed experiment. The incident energy assumed is  $E_i = 11.0$  GeV. The electron kinematics is held fixed at  $x_{bj} = 1.35$  and  $Q^2 = 4.25(\text{GeV}/c)^2$ .

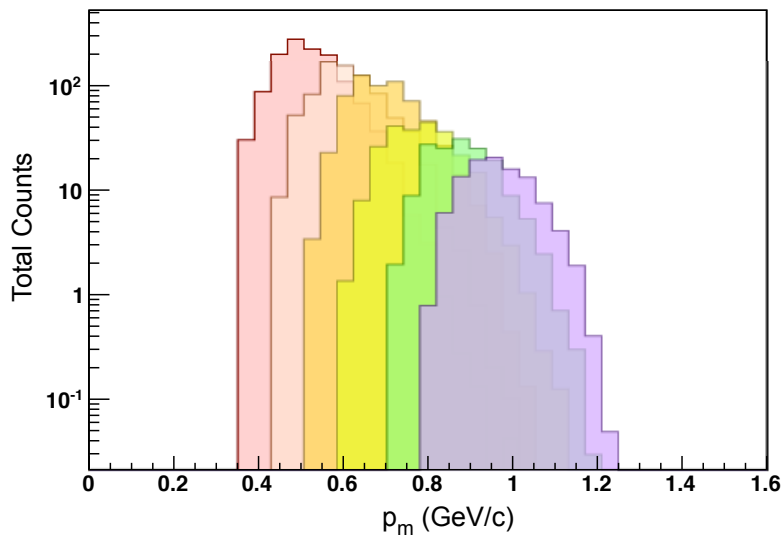


Figure 10: Acceptance in missing momentum for the proposed kinematic settings. The cuts described in the section on count rates have been applied.

Clearly the different settings have considerable overlap. We plan to use this overlap to obtain a continuous data set of cross sections between a missing momentum of 0.5 and 1.0 GeV/c. The estimated statistical errors of the data are indicated in Fig. 12. We expect that this experiment is dominated by the statistical error since one typically obtains a systematic error of the order of 5%. The expected statistical errors range from 5% for the lower missing momenta to 20% for 1.0 GeV/c. Given that this kinematic region can be considered as an unexplored new territory we believe that a 20% measurement is still very valuable.

## 4 Count-Rates

The coincidence count-rates for electrons in SHMS and protons in HMS have been estimated using the Hall-C monte-carlo program SIMC [43]. The coincidence cross section has been calculated within the PWIA using the V18 momentum distribution and included radiative effects. The following cuts have been applied for the rate estimates:

**electron solid angle :**  $-0.05 \leq \vartheta_e \leq 0.05$ ,  $-0.025 \leq \varphi_e \leq 0.025$ ,  
angles are in radians

**electron momentum acceptance :**  $-0.08 \leq \Delta p/p \leq 0.04$

**proton solid angle:**  $-0.06 \leq \vartheta_p \leq 0.06$ ,  $-0.035 \leq \varphi_p \leq 0.035$

**proton momentum acceptance :**  $-0.1 \leq \Delta p/p \leq 0.1$

**Bjorken-x:**  $1.3 \leq x_{bj} \leq 1.4$

**missing momentum :** missing momentum bin width =  $\pm 0.02$  GeV/c

**missing energy :**  $-10 \leq \epsilon_m \leq 25$  MeV

**momentum transfer :**  $Q^2 = 4.25 \pm 0.25$  (GeV/c)<sup>2</sup>

A 15 cm liquid deuterium target and a current of  $80\mu\text{A}$  have been assumed, which results in a luminosity of  $L = 3.2 \cdot 10^{38}$   $\text{cm}^2 \cdot \text{sec}^{-1}$ . The results of these estimates are shown in Fig. 11 in which the counts per hour (after combining different HMS settings) are plotted as a function of missing momentum. In Fig. 12, the estimated statistical errors are compared to calculated cross sections using different models for the deuteron wave function and final state interactions.

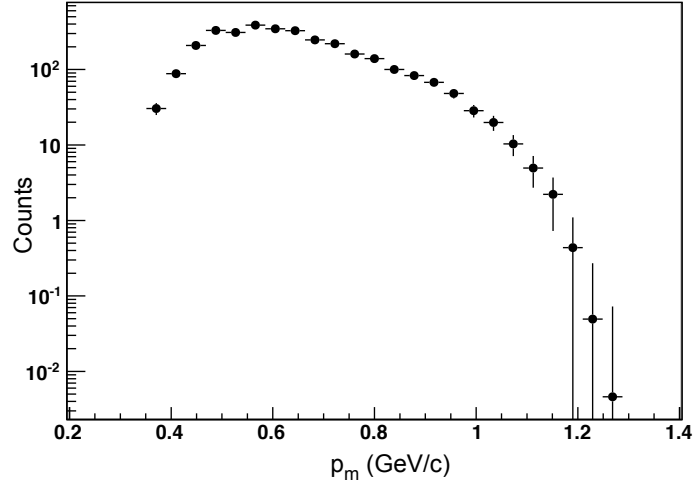


Figure 11: Total counts expected per missing energy bin. Included are all the cuts described in this section and overlapping kinematic settings have been added.

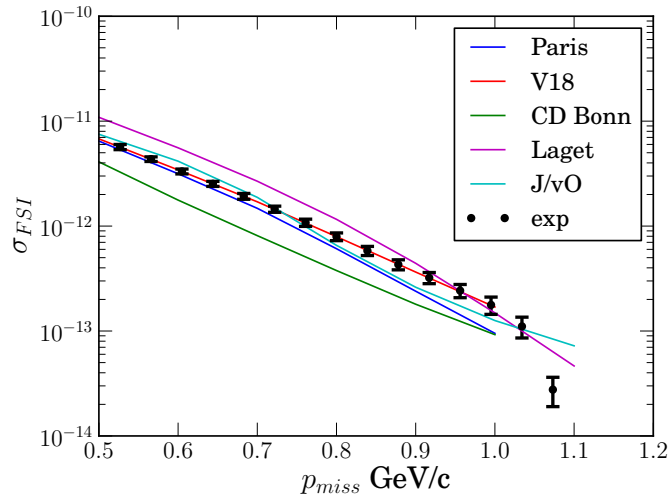


Figure 12: The expected statistical error as a function of missing momentum compared to a range of calculations including FSI and different models for the deuteron wave function.

The proposed electron kinematics differs from the one of the previous D(e,e'p)n experiment (E01-020) in that the momentum transfer has increased from 3.5 to 4.25 (GeV/c)<sup>2</sup> and the incident energy has been doubled. The singles rates measured previously in E01-020 were about 1 KHz for electrons and about 400 Hz for protons for the  $p_m = 0.5$  GeV/c setting. The inclusive electron scattering code INCLUSIVE by M.Sargsian [44], which reproduces inclusive cross sections quite well, has been used to estimate the electron singles rates for the new kinematics. The results showed that the rates are very similar to those of the Hall A experiment. We therefore expect similar electron singles rates and similar or lower proton rates for the proposed kinematics. No corrections for accidental coincidences were necessary in the analysis of the  $Q^2 = 3.5$  (GeV/c)<sup>2</sup> kinematics of E01-020 data, due to the small single rates (Fig. 13).

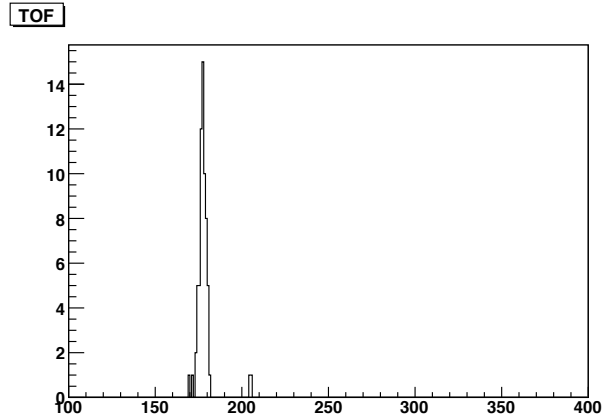


Figure 13: Time of flight spectrum between the two spectrometers as obtained in the E01-020 experiment for  $Q^2 = 3.5$  (GeV/c)<sup>2</sup>,  $p_m = 0.5$  GeV/c and  $x_{bj} \approx 1.45$ .

Using the code EPC to estimate the variation of the proton singles rate at the spectrometer settings for the higher missing momenta measurements, we found that it is expected to increase by a factor of 1.6 for the highest missing momentum setting. At this setting the overall signal to noise ratio, using the full acceptance of the spectrometers, a timing window of 2.5 ns, and without a cut in missing energy was estimated to be 1:1 and we expect this ratio to be much higher once all cuts have been applied.

Proton and electron singles rates are well within the capabilities of the spectrometer detector systems. The resulting signal to noise ratio is generally

large and we do not anticipate any background problems. In E01-020 we found the pion rates to be generally well below the singles rates for electron and protons. In the electron arm, pions will be rejected by using the calorimeter and the noble gas Cherenkov detector. In the hadron arm, pions can be rejected using time-of-flight measurements since the momenta involved are below 2.3 GeV/c and the corresponding time-of-flight difference between pions and protons is  $\geq 5.8$  ns. In addition pion events produce a continuous missing energy spectrum and no significant pion background has been found in the previous experiment.



## 5 Beam Time Request

We plan to measure a total of 9 different kinematic settings (including the hydrogen elastic calibrations). Table 2 shows the summary of the requested beam time. The beam time on target required to achieve the necessary statistics includes the following items:

- Time to determine the spectrometer pointing at each setting
- Time for target and spectrometer changes

The two low  $p_m$  measurements are calibration measurements that overlap with the Hall A experiment.

$p_m$ GeV/c	Data Taking	Overhead	Sub-total
0.1 ( $Q^2 = 3.5$ (GeV/c) <sup>2</sup> )	3.75	2.0	5.75
0.1	3.75	2.0	5.75
0.5	40.63	2.0	42.63
0.6	46.75	2.0	48.75
0.7	66.88	2.0	68.88
0.8	59.38	2.0	61.38
0.9	82.00	2.0	84.00
1.0	136.75	2.0	138.75
Optics Commissioning			16
Target Commissioning			16
<sup>1</sup> H(e,e'p) calibrations	2.0	4.0	6.0
TOTAL			488.13

Table 2: Beam Time Overview

## References

- [1] K. S. Egiyan *et al.* [CLAS Collaboration], Phys. Rev. C **68**, 014313 (2003).
- [2] K. S. Egiyan *et al.* [CLAS Collaboration], Phys. Rev. Lett. **96**, 082501 (2006).

- [3] R. Shneor *et al.* [Jefferson Lab Hall A Collaboration], *Phys. Rev. Lett.* **99**, 072501 (2007).
- [4] R. Subedi *et al.*, *Science* **320**, 1476 (2008).
- [5] S. Jeschonnek and J. W. Van Orden, *Phys. Rev.*, **C 78**, 014007 (2008)
- [6] S. Jeschonnek and J. W. Van Orden, *Phys. Rev. C* **80**, 054001 (2009).
- [7] S. Jeschonnek and J. W. Van Orden, arXiv:0911.3629 [nucl-th].
- [8] J. M. Laget, *Phys. Lett. B* **609**, 49 (2005).
- [9] C. Ciofi degli Atti and L. P. Kaptari, *Phys. Rev. Lett.* **100**, 122301 (2008).
- [10] M. M. Sargsian, arXiv:0910.2016 [nucl-th].
- [11] P.E Ulmer, *et al.*, *Phys. Rev. Lett.*, **89**, 062301 (2002).
- [12] Egiyan K Sh, Griffioen K A and Strikman M I (spokespersons) 1994 Measuring Nuclear Transparency in Double Rescattering Processes *Jefferson Lab Proposal E94-019*.
- [13] Boeglin W, Jones M, Klein A, Mitchell, Ulmer P and Voutier E (spokespersons) 2001 Short-Distance Structure of the Deuteron and Reaction Dynamics in  $^2\text{H}(e,e'p)n$  *Jefferson Lab Proposal E01-020*.
- [14] K. S. Egiyan *et al.* [the CLAS Collaboration], *Phys. Rev. Lett.* **98**, 262502 (2007).
- [15] L. L. Frankfurt, M. M. Sargsian and M. I. Strikman, *Phys. Rev. C* **56**, 1124 (1997)[arXiv:nucl-th/9603018].
- [16] M. M. Sargsian, *Int. J. Mod. Phys. E* **10**, 405 (2001) [arXiv:nucl-th/0110053].
- [17] S. Jeschonnek, *Phys. Rev. C* **63**, 034609 (2001) [arXiv:nucl-th/0009086].
- [18] J. M. Laget, *Phys. Lett. B* **609**, 49 (2005).
- [19] C. Ciofi degli Atti, L. P. Kaptari and D. Treleani, *Phys. Rev. C* **63**, 044601 (2001) [arXiv:nucl-th/0005027].
- [20] J.M. Laget, *private communication*.
- [21] S. Jeschonnek, *private communication*.

- [22] W. Van Orden *private communication*.
- [23] C. Ciofi degli Atti, *private communication*.
- [24] M.M. Sargsian, *private communication*.
- [25] H. Arenhoevel, *private communication*.
- [26] S. Jeschonnek (contact person), *Deuteron Benchmarking Collaboration*.
- [27] V.R. Pandharipande and S.C. Pieper, Phys. Rev. C **45**, 791 (1992).
- [28] T. De Forest, Nucl. Phys. A **392**, 232 (1983).
- [29] J. . J. Adam, F. Gross, S. Jeschonnek, P. Ulmer and J. W. Van Orden, Phys. Rev. C **66**, 044003 (2002).
- [30] C. Bochna *et al.*, Phys. Rev. Lett. **81**, 4576 (1998).
- [31] E.C. Schulte *et al.*, Phys. Rev. Lett. **87**, 102302 (2001).
- [32] E. C. Schulte *et al.*, Phys. Rev. C **66**, 042201 (2002).
- [33] M. Mirazita *et al.*[CLAS Collaboration], Phys. Rev. C **70**, 014005 (2004)
- [34] R. A. Gilman and F. Gross, J. Phys. G **28**, R37 (2002).
- [35] S.J. Brodsky and J.R. Hiller, Phys. Rev. C **28**, 475 (1983).
- [36] L. A. Kondratyuk *et al.*, Phys. Rev. C **48**, 2491 (1993); V. Y. Grishina, *et al.* Eur. Phys. J. A **10**, 355 (2001).
- [37] L.L. Frankfurt, G.A. Miller, M. M. Sargsian and M. I. Strikman, Phys. Rev. Lett. **84**, 3045 (2000).
- [38] M. M. Sargsian *et al.*, J. Phys. G **29**, R1 (2003) [arXiv:nucl-th/0210025].
- [39] K.I. Blomqvist *et.al.*, Phys. Lett.**B429** (1998) 33.
- [40] T.G. O'Neill *et al.*, Phys. Lett. **B351** (1995) 87.
- [41] J.-E. Ducret *et.al.*, Phys. Rev. **C49** (1994) 1783.
- [42] L. Coman, *Phd Thesis, FIU, August 2007*.
- [43] Computer Program SIMC.
- [44] Computer Program INCLUSIVE, M.Sargsian,*CLAS-NOTE 90-007* (1990).